Declutching control of a wave energy converter

A. Babarit, Michel Guglielmi, A.H. Clement

Declutching control of a Wave Energy Converter

Aurélien Babarit[a], Michel Guglielmi[b], Alain H. Clément[a]

[a] *Laboratoire de Mécanique des Fluides (CNRS UMR6598)*
Ecole Centrale de Nantes, 1 Rue de la Noë B.P 92101 44321 Nantes cedex 3, France.
[b] *Institut de Recherche en Communication et Cybernétique de Nantes(CNRS UMR6597)*
Ecole Centrale de Nantes, 1 Rue de la Noë B.P 92101 44321 Nantes cedex 3, France.

Abstract

When hydraulic Power Take Off (PTO) is used to convert the mechanical energy of a wave energy converter into a more useful form of energy, the PTO force needs to be controlled. Continuous controlled variation of the PTO force can be approximated by a set of discrete values. This can be implemented using either variable displacement pumps or several hydraulic cylinders or several high pressure accumulators with different pressure levels. This pseudo continuous control could lead to a complex PTO with a lot of components. A simpler way for controlling this hydraulic PTO is declutching control, which consists in switching on and off alternatively the wave energy converter's PTO. This can be achieved practically using a simple by-pass valve. In this paper, the control law of the valve is determined by using the optimal command theory. It is shown that, theoretically when considering a wave activated body type of WEC, declutching control can lead to energy absorption performance at least equivalent to that of pseudo-continuous con-

Email addresses: aurelien.babarit@ec-nantes.fr (Aurélien Babarit), michel.gulgliemi@irccyn.ec-nantes.fr (Michel Guglielmi), alain.clement@ec-nantes.fr (Alain H. Clément)

trol. The method is then applied to the case of the SEAREV wave energy converter, and it is shown than declutching control can even lead to a higher energy absorption, both in regular and irregular waves.
Key words: wave energy converter, declutching control, hydraulic power take off, optimal command

---

Introduction

Amongst the wide variety of Wave Energy Converter (WEC) concepts that have been proposed, the class of so-called *wave activated bodies* WECs uses wave induced motions of masses or large bodies to drive a Power Take Off (PTO) system which transforms the primary mechanical energy of the body into a final usable form, generally electricity. A lot of devices are based on this concept, such as for example the WRASPA [Chaplin 2007], the SEAREV [Josset 2007], or the Pelamis [Henderson 2006] whose first units have been deployed into Scottish and Portuguese waters.

In many cases [Henderson 2006], [Josset 2007], the PTO is hydraulic. It usually features one or several hydraulic cylinders, high pressure accumulators and a hydraulic motor which drives an electrical generator. Figure (1) shows a typical hydraulic PTO system. This seems to be a reasonable option, at least at a prototype stage. There are many of the shelf hydraulic components from the marine and offshore industry that are capable of dealing with the large forces and slow motions usually occuring in wave energy conversion. Moreover, high pressures accumulators allow storage of the energy extracted from the waves, and thus contribute to the smoothing of the output power delivered to the grid.

Figure 1. Schematic representation of a hydraulic power take off for wave energy conversion.

When designing such hydraulic PTOs, it is necessary to include components allowing control of the force applied by the PTO to the prime mover of the wave energy converter. In contrast with the smooth continuous force applied by a linear damper, the force of a hydraulic PTO is a Coulomb damping. This means that its modulus is a constant equal to the area of the cylinder times the pressure difference between the high pressure (HP) and low pressure (LP) accumulators. When the pressure difference between the accumulators is too large, the PTO force can cancel the other external forces (including the wave excitation force), hence preventing any motion of the wave energy converter, which would result in a zero energy production. On the other hand, if the pressure difference is too small, the PTO force can become too small in comparison with what it should be to maximise the energy absorption or to keep the amplitude of the motion in an acceptable range.

These effects were observed by [Falcao 2007] on a generic heaving WEC and by [Josset 2007] on the SEAREV WEC. It was found by both authors that they can be counteracted using a slow control method consisting in adapting the pressure in the HP accumulator and the flow in the hydraulic motor to the sea state. By using this *sea state dependent control*, it was even found that the output power can sometimes exceed that of an optimised linear damping PTO. In [Falcao 2008], it is shown that phase control can

successfully be achieved for a heaving buoy WEC with a hydraulic PTO using a similar sea state dependent control. In this case, the control consists in adapting the flow in the hydraulic motor and the flow from the hydraulic cylinder.

By using several hydraulic cylinders and/or several HP accumulators with different pressure levels in the hydraulic PTO, it is also possible to control the PTO force in order to adapt it to each incoming wave and it is even possible to mimic a continuous behaviour, as it seems to be done in the Pelamis for example [Henderson 2006]. Later in this paper, this strategy for controlling the PTO force will be called *pseudo-continuous control*. In comparison with the sea state dependent control strategies, it brings a lot more complexity in the PTO, raising technical issues such as a possibly higher risk of failure.

As an alternative to this, we consider another strategy of *declutching control*, or unlatching as it was introduced by [Salter 2002]. It consists in declutching the PTO - which means that the PTO force is set equal to 0 - during some parts of the cycle. Technologically, it is very simple to implement, as it needs only a by-pass valve in the circuit of the hydraulic cylinder. This control has already been considered by [Justino 2000] for the Portuguese oscillating water column in Pico : the relief valve was intended to control the air flow through the Wells turbine in order to prevent it from exceeding the aerodynamic stall-free range, and in this way reduce aerodynamic losses in the turbine. However, it was not considered as a mean of controlling the PTO force.

There are many other ways of controlling the PTO force of a wave energy converter and one can refer to [Salter 2002] for an exhaustive review of all

of them. However, we chose to focus here only on both pseudo-continuous control and declutching control beacuse our aim is to show that, at least theoretically, pseudo-continuous control can be advantageously replaced by declutching control. Indeed, we show here that there is actually no need for a complex hydraulic PTO featuring several HP accumulators or several hydraulic cylinders as only one by-pass valve is conceptually sufficient in order to achieve at least the same level of energy absorption. This is shown theoretically in the first part of this paper by applying the optimal command theory to the generic equations of floating wave energy converters, including the hydraulic PTO. Then, the method is applied to the SEAREV WEC as an example, and theoretical results are confirmed.

1. Governing equations

1.1. Equation of motion

Let us consider a generic wave energy converter composed of one or several bodies moving under the action of incident waves. Let N_{dof} be the total number of degrees of freedom of this wave energy converter. Assuming the fluid to be non-viscid and incompressible, the flow to be irrotationnal and the amplitude of motions and waves to be sufficiently small compared to the wavelength , the classical linearized potential theory can be used as a framework for calculation of the fluid-structure interactions. Hence, one can write the equation of motion of the WEC in the time domain as:

$$\left(\mathbf{M}+\left[\mu_{\infty}\right]\right)\ddot{\mathbf{Y}}+\int_{0}^{t}\mathbf{K_{rad}}\left(t-\tau\right)\dot{\mathbf{Y}}\left(\tau\right)d\tau+\left(\mathbf{K}_{H}+\mathbf{K}_{A}\right)\mathbf{Y}=\mathbf{F}_{ex}+\mathbf{F}_{PTO}$$

(1)

with:

- $\mathbf{Y}, \dot{\mathbf{Y}}, \ddot{\mathbf{Y}}$ being respectively the generalized position, velocity and acceleration vectors of the WEC.
- $\mathbf{M}$ the generalized mass matrix of the system.
- $\mathbf{K}_H$ the hydrostatic stiffness matrix of the system.
- $\mathbf{K}_A$ an additional stiffness matrix which represents the action of moorings.
- $[\mu_\infty]$ the added mass matrix and $\mathbf{K_{rad}}$ the radiation impulse response matrix which represents the radiation of waves by the body after an impulsive velocity at $t = 0$, according to the classical Cummins' decomposition [Cummins 1962]. Using Prony's method [Duclos 2001], one can further approximate each of the $K_{rad,kl}$ functions, components of $\mathbf{K_{rad}}$, by a sum of N_{kl} complex functions $K_{rad,kl}(t) = \sum_{j=1}^{N_{kl}} \sigma_{klj} exp(i\beta_{klj}t)$. As a consequence of this approximation by series of exponential functions, each convolution product can be replaced by a sum of N_{kl} additionnal *radiative* complex states $\int_0^t K_{kl}\left(t-\tau\right)\dot{Y}_l\left(\tau\right)d\tau = \sum_{j=1}^{N_{kl}} I_{klj}$ with each I_{klj} given by an ordinary differential equation $\dot{I}_{klj} = \beta_{klj} I_{klj} + \sigma_{klj}\dot{Y}_l$.

Finally, one can get :

$$\int_0^t \mathbf{K_{rad}}\left(t-\tau\right)\dot{\mathbf{Y}}\left(\tau\right)d\tau = [\delta]\mathbf{I}$$

$$\dot{\mathbf{I}} = [\beta]\mathbf{I} + [\sigma]\dot{\mathbf{Y}} \tag{2}$$

with $\mathbf{I} = \left(I_{klj}\right)_{1\leq k\leq N_{dof},1\leq l\leq N_{dof},1\leq j\leq N_{kl}}$. More details on this method can be found in [Babarit 2006].

- $\mathbf{F}_{ex}$ is the excitation vector, associated to the action of incident and diffracted wave fields upon the WEC. Using King's approach [King 1987], let $\mathbf{K}_{ex}\left(t\right)$ be the force response associated to an impulsive elevation on the free surface propagating along the x axis. Using the superposition principle, owing to the global linearity of the problem solved here, the generalized excitation force is then given by

$$\mathbf{F}_{ex}\left(t\right) = \int_0^t \mathbf{K}_{ex}\left(t-\tau\right)\eta\left(\tau\right)d\tau \tag{3}$$

with $\eta(t)$ being the free surface elevation at a given reference location. In case of regular wave, $\eta(t)$ is an elementary sine function $a\sin(\omega t+\varphi)$ with a the amplitude of the wave, ω its circular frequency and φ an initial phase. In case of random waves, $\eta(t)$ will be considered here as a sum of N_c elementary sinus functions whose amplitudes $\left(a_j\right)_{j=1,N_c}$ are derived from the standard Pierson-Moskowitz energy spectrum [Molin 2002] and whose phases $\left(\varphi_j\right)_{j=1,N_c}$ are set randomly.

- $\mathbf{F}_{PTO}$ is the force vector associated to the action of the power take off. If the PTO is a linear damper, $\mathbf{F}_{PTO}$ is given by :

$$\mathbf{F}_{PTO} = \mathbf{B}_{PTO}\dot{\mathbf{Y}}$$

with $\mathbf{B}_{PTO}$ being the PTO damping coefficient matrix.

1.2. Equation for the PTO

A linear damper is the classical basic approach for modeling the PTO of a wave energy converter, leading to a global solution of the equation of motion in the frequency domain. But in the real world, a hydraulic PTO system is composed of non linear components such as the accumulator, which requires to solve the problem in the time domain.

Let us consider here the typical hydraulic PTO shown in figure (1). It is composed of a hydraulic cylinder, a high pressure accumulator, a low pressure fluid tank and a hydraulic motor coupled to a generator. The displacement of the hydraulic motor is chosen variable, allowing a control of the output flow from the HP accumulator. Let $p(t)$ be the pressure in the HP accumulator, let $V(t)$ be its volume of gas. Let p_0 be the pressure in the LP accumulator. We assume that the volume of the LP accumulator is large enough for its pressure to remain constant. Let S_c the cross-sectional area of the cylinder and v_m the maximum displacement of the variable displacement hydraulic motor.

With these notations, the fluid flow from the high pressure accumulator to the hydraulic motor is $q_m = u_m v_m \Omega$, with Ω the rotational velocity of the motor and $u_m \in [0, 1]$ the control variable on the displacement of the motor. Let J be the index of the degree of freedom driving the motion of the hydraulic cylinder. The flow from the cylinder to the high pressure accumulator is $q_p = u_c S_c |\dot{Y}_J|$, in which u_c is the control variable for the cylinder. If u_c is set equal to 1, the cylinder is either fully operating, pumping oil into the high pressure accumulator; either locked in position because the

PTO force exceeds the hydrodynamic force. If u_c is equal to 0, the cylinder is by-passed. In the latter case, the cylinder is declutched from the WEC and the mechanical energy of the system is not extracted.

The variation of the gas volume in the high pressure accumulator is given by the sum of the flow coming from the cylinder plus the flow going out to the hydraulic motor:

$$\dot{V} = q_p + q_m = -u_c S_c |\dot{Y}_J| + u_m v_m \Omega \tag{4}$$

We assume the compression in the high pressure accumulator to be isentropic, which leads to:

$$\dot{p} = -\gamma p \frac{\dot{V}}{V} \tag{5}$$

with $\gamma = 1.4$ in case of nitrogen.

When $|\dot{Y}_J| > 0$, the J^{th} component of the PTO force applied to the WEC is:

$$F_{PTO,J} = -u_c S_c (p - p_0) \text{sign}(\dot{Y}_J) \tag{6}$$

since $\dot{Y}_J$ is the component of the velocity vector corresponding to the velocity of the cylinder by definition of index J. When $|\dot{Y}_J| = 0$, equation (6) is no longer applicable. Two cases can occur: either the pressure in the HP accumulator is too high for the hydraulic cylinder to be able to operate and then the acceleration of the productive motion $|\ddot{Y}_J|$ is also equal to 0; or it is not, and then $|\ddot{Y}_J| > 0$.

In the first case, since $|\ddot{Y}_J| = 0$, the value of the PTO force can be deduced from equation (1). So, $F_{PTO,J} = -F_{h,J}$ in which $\mathbf{F}_{h,J}$ is the force vector associated with the sum of all forces (including inertia forces) acting on the system except the PTO force $\mathbf{F}_h = \mathbf{F}_{ex} - [\delta]\mathbf{I} - (\mathbf{K}_H + \mathbf{K}_A)\mathbf{Y} - (\mathbf{M} + [\mu_\infty])\,\ddot{\mathbf{Y}}$.

In the second case, since $|\ddot{Y}_J| > 0$, $|F_{PTO,J}| = u_c S_c(p - p_0)$ and one can show that the sign of $F_{PTO,J}$ is the opposite of the sign of $F_{h,J}$.

Finally, when $|\dot{Y}_J| = 0$, one can write:

$$F_{PTO,J} = -\min\left(|F_{h,J}|, u_c S_c(p - p_0)\right) \operatorname{sign}(F_{h,J}) \tag{7}$$

1.3. State equation.

Using equations (4), (5), (1), (2) and given control laws for the control variable u_c of the hydraulic cylinder and u_m the hydraulic motor, one can simulate numerically the full behaviour of the wave energy converter, including its PTO. However, in order to be able to use the optimal command method later in this paper, the equation of motion is re-written under a classical state equation form.

Let

$$\mathbf{X} = \begin{pmatrix} \mathbf{Y} & \dot{\mathbf{Y}} & V & p & \mathbf{I} \end{pmatrix}^t \tag{8}$$

be the extended state vector. Using equations (1), (2), (4) and (5), one can write:

$$\dot{\mathbf{X}} = \mathbf{f}(\mathbf{X}, u_c, u_m) \tag{9}$$

with $\mathbf{X}(0) = \mathbf{X}_0$ and $\mathbf{f}(\mathbf{X}, u_c, u_m)$ as given in appendix.

1.4. Equations for the control

1.4.1. Control of the hydraulic motor u_m.

The instantaneous power absorbed by the hydraulic power take off is $P_{PTO} = \mathbf{F}_{PTO}^t \dot{\mathbf{Y}}$. Using equations (6) and (7), one can re-write it $P_{PTO} = -u_c S_c(p - p_0)|\dot{Y}_J|$ whatever $|\dot{Y}_J|$.

The energy extracted from the waves over the time range $[t-\Delta t, t]$ is $E = \int_{t-\Delta t}^{t} P_{PTO}(\tau)d\tau$. The instantaneous power delivered to the grid by the hydraulic motor is $P_m = (p-p_0)u_m v_m \Omega$. In order to smooth the electricity produced, the control variable u_m is determined such that the instantaneous power produced by the motor is equal to the "instantaneous" mean power extracted from the waves over the time window Δt:

$$u_m v_m \Omega (p-p_0)\Delta t = E \tag{10}$$

In this study, Δt is set equal to the whole duration of the simulation because the sea state does not change during the simulations. In real sea situations, one should set the time window according to the temporal coherence of the sea state.

1.4.2. Pseudo-continuous control of the PTO force.

In this study, we consider first a pseudo-continuous control aiming at mimicking a continuous force $\mathbf{F}_{con}(t)$, as shown in figure (2). Notice that, at this point of the paper, there are no restrictions on the mathematical expression of this continuous force. In particular, it could include a term proportional to the velocity of the hydraulic cylinder, but also a reactive part proportional to its position or acceleration.

Figure 2. Principle of the pseudo-continuous control of the force of a hydraulic PTO.

One can imagine achieving this pseudo-continuous control by means of several by-pass valves coupled with several HP accumulators with different

pressure levels or several hydraulic cylinders, or even directly by using a pump with variable displacement such as the Digital Displacement pump developed by the company Artemis Intelligent Power for example. Whatever the technical solution, one can write the PTO force as follows:

$$|F_{PTO}| = u_c S_c (p - p_0) \tag{11}$$

with $u_c \in \left\{u_1, u_2, \ldots, u_{N_q}\right\}$ the N_q discrete control levels for the PTO force such as $\forall 1 \leq q \leq N_q$, $u_q \in [0, 1]$ and with u_1 and u_{N_q} being such as $u_1 = 0$ and $u_{N_q} = 1$. In the case of several hydraulic cylinders, S_c would be the maximal area achievable (i.e all hydraulic cylinders working together) and in the case of several HP pressure accumulators, p would be the highest pressure.

Without any loss of generality, one can assume $u_1 \leq u_2 \leq \ldots \leq u_{N_q}$. At time t, the value of the control variable is then given by :

$$u_c = u_q \quad \text{with } q/ \quad u_q \leq \frac{\mathbf{F}_{con}(t)}{S_c(p - p_0)} < u_{q+1} \tag{12}$$

Notice that when $\mathbf{F}_{con}(t) > S_c(p - p_0)$, the control variable saturates at $u_c = 1$.

1.4.3. Declutching control

Following [Babarit 2006], one can use the optimal command theory based on Pontryagin principle [Hoskin 1986] in order to compute control law for u_c which maximises the extracted energy from the waves over a given time interval.

Let define the optimisation problem:

$$\max_{u_c} E = -\int_0^{t_f} P_{PTO} d\tau \tag{13}$$

with $u_c \in [0, 1]$

We define the hamiltonian $H(t)$:

$$H = -P_{PTO} + \mathbf{\Lambda}^t \mathbf{f} \tag{14}$$

with $\mathbf{\Lambda}$ the adjoint states vector. One can show that, when $|\dot{Y_J}| > 0$, it is linear with respect to the control variable u_c :

$$H = u_c \text{sign}(\dot{Y_J}) h(\mathbf{X}, \mathbf{\Lambda}) + g(\mathbf{X}, \mathbf{\Lambda}) \tag{15}$$

with g and h scalar functions depending on both $\mathbf{X}$ and $\mathbf{\Lambda}$. Their formulas are given in appendix.

When $|\dot{Y_J}| = 0$, it is given by:

$$H = \min\left(|F_{h,J}|, u_c S_c(p - p_0)\right) \text{sign}(F_{h,J}) h(\mathbf{X}, \mathbf{\Lambda}) + g(\mathbf{X}, \mathbf{\Lambda}) \tag{16}$$

From the maximum principle [Borne et al. 1990], the command is optimal when it maximizes the hamiltonian H. Hence, the equation for the control variable $u_c(t)$ is:

$$u_c = \begin{cases} \max\limits_q u_q & \text{if} \quad \text{sign}(\dot{Y_J}) h(\mathbf{X}, \mathbf{\Lambda}) > 0 \\ \min\limits_q u_q & \text{else} \end{cases} \tag{17}$$

when $|\dot{Y_J}| > 0$ and:

$$u_c = \begin{cases} \max\limits_q u_q & \text{if} \quad \text{sign}(F_{h,J}) h(\mathbf{X}, \mathbf{\Lambda}) > 0 \\ \min\limits_q u_q & \text{else} \end{cases} \tag{18}$$

when $|\dot{Y_J}| = 0$.

Since we assumed that $\max_q u_q = 1$ and $\min_q u_q = 0$, these criteria can be rewritten:

$$u_c = \begin{cases} 1 & \text{if} \quad \text{sign}(\dot{Y}_J) h(\mathbf{X}, \mathbf{\Lambda}) > 0 \quad \text{and} \quad |\dot{Y}_J| > 0 \\ 1 & \text{if} \quad \text{sign}(F_{h,J}) h(\mathbf{X}, \mathbf{\Lambda}) > 0 \quad \text{and} \quad |\dot{Y}_J| = 0 \\ 0 & \text{else} \end{cases} \tag{19}$$

From this last equation, it follows that :

- the optimal value for the control variable u_c is either 0 either 1, depending on the criterion of equation (19). Thus, **intermediate states for the control variable u_c in the range $]0, 1[$ are never reached as optimal values**. This means that the force applied by the PTO on the WEC should be either a zero force or the maximum force available and that pseudo-continuous control is not an optimal way for controlling the system. In other words, this shows that there is no need for several HP accumulators working at different pressure levels or several hydraulic cylinders, since at least an equivalent level of energy can theoretically be absorbed using:

  1. only one HP pressure accumulator with the highest pressure
  2. only one hydraulic cylinder whose area is S_c
  3. declutching control with an optimal command.

- When relative velocity of the cylinder reaches zero, the value of the control variable u_c can behave in two ways. If the cylinder velocity just before it reaches zero and the force $F_{h,J}$ are of opposite sign, then the value of u_c changes immediately. Otherwise, this change is delayed until the sign of $\text{sign}(F_{h,J}) h(\mathbf{X}, \mathbf{\Lambda})$ changes. Either way, these changes are

smooth for the PTO as they occur when the velocity is zero. However, the other changes, occuring when $|\dot{Y}_J| > 0$ and determined by the zero crossings of the function h, may lead to high stress levels of the mechanical components of the PTO since they could happen when the velocity is high. For a practical application of declutching control, this should be taken into consideration in the sizing of the PTO.

Finally, we need a last equation for describing the behaviour of the adjoint state vector $\mathbf{\Lambda}$. According to [Borne et al. 1990], it is given by :

$$\dot{\mathbf{\Lambda}} = -\frac{\partial H}{\partial \mathbf{X}} \tag{20}$$

with $\mathbf{\Lambda}(t_f) = 0$ as we chose the final condition $\mathbf{X}(t_f)$ to be free.

2. Application to the SEAREV wave energy converter

The SEAREV wave energy converter is a floating device completely closed fitted with a large and heavy pendular wheel as shown in figure (3). Under waves action, the hull and the wheel start to move, each one with its own motion. The relative motion α between the floating device and the wheel is used to drive the hydraulic power take-off consisting of two radial piston pumps, of a high pressure accumulator, of a variable displacement hydraulic motor and of a low pressure oil tank (see figure (4)).

Figure 3. Schematic representation of the SEAREV wave energy converter and notations used.

Figure 4. Schematic representation of the hydraulic PTO of the SEAREV wave energy converter. A radial piston pump is used instead of a hydraulic cylinder.

The equation of motion of the SEAREV with its hydraulic PTO was written under the form of equation (9) in a previous study [Josset 2007]. Computation of the hydrodynamic coefficients $[\mu_\infty]$ and the impulse response functions $\mathbf{K_{rad}}$ and $\mathbf{K}_{ex}$ was done using the BEM code ACHIL3D [Clément 1997]. Characteristics of the SEAREV's PTO are given in table (1).

Table 1. Characteristics of the SEAREV's hydraulic PTO.

A Runge-Kutta 2nd order scheme is used to integrate the equation of motion in order to perform time domain simulations of the SEAREV WEC. In case of pseudo-continuous control, we chose to mimic the behaviour of a linear damper, i.e $F_{PTO} = -B_{PTO}\dot{\alpha}$, in which the damping coefficient B_{PTO} was optimised in a previous study [Babarit 2005]. Practically, u_c is discretised in N_q discrete values $u_q = \frac{q-1}{N_q-1}$ and u_q is calculated at each time step according to equation (12). An example of the PTO force applied on the SEAREV when using this pseudo-continuous control with $N_q = 10$ is shown in figure (5).

Figure 5. Comparison of the PTO force achieved with the SEAREV's hydraulic PTO controlled with the pseudo-continuous control and the PTO force achieved with a linear damper. In this example, the PTO force is dis-

cretised in 10 levels.

In case of declutching control, an iterative scheme following [Babarit 2006] is used to compute the optimal control law for u_c. First, the equation of motion is computed by integrating equation (9) forward for $t \in [0, t_f]$. Then, once the motion has been determined, the adjoint state vector can be computed by integrating backwards equation (20) from $t = t_f$ to $t = 0$. Knowing both $\mathbf{X}$ and λ, one can deduce a new control law at each time step according to equation (19), and then iterate the process.

This scheme can be difficult to implement in practice because it needs the knowledge of the future of the excitation force, which requires prediction of the incoming wave. This could be done using various techniques, such as Kalman filtering (successfully used by Budal et al. in [Budal and Falnes 1983]) or wave propagation numerical model (promising results of deterministic wave propagation have been reported recently in [Blondel 2008]) for example. However, these considerations are beyond the scope of this study, in which the optimal command method with the iterative scheme described above is used in order to achieve comparisons between the energy absorbed with pseudo-continuous control and declutching control.

2.1. Regular waves

Figure (6) shows a result of a time domain simulation of the motion of the SEAREV WEC with pseudo-continuous control and with declutching control. In this simulation, the parameter N_q was set equal to 10 and the incident waves are regular. Its period is 8.2 seconds and its amplitude 0.5 meter. For such a simulation, the required CPU time is a few minutes on a

3.4GHz Pentium(R) PC.

Figure 6. Time domain simulation of the motion of the SEAREV WEC with a hydraulic PTO controlled with the pseudo-continuous control (solid line) and with declutching control (dashed line). From top to the bottom, the figure shows the incoming wave, the relative motion of the wheel, the PTO force and the absorbed energy from the waves. In this example, the wave period is 8.2 seconds and the wave amplitude is 0.5 meter.

One can see in this figure that the amplitude of the relative (productive) motion jumps from about 10 degrees with the pseudo-continuous control to more than 40 degrees with the declutching control. At the same time, the amplitude of the PTO force is amplified by a factor of about 3. In the bottom figure, one can see that the cumulative effect of the amplification of the amplitude of the motion and the PTO force results finally in a doubling of the extracted energy from the waves.

Figure 7. PTO force with declutching control and velocity of the relative motion between the hull and the pendular wheel. One can observe that each zero-crossing of the velocity leads to a change in the state of the controller from declutching to operating.

In order to achieve a better understanding of the behaviour of the PTO when it is controlled using declutching, we plotted in the same figure (7) the velocity of the relative motion of the wheel and the PTO force. One

can observe that each zero-crossing of the velocity leads to a change in the controller state. This corresponds to what was found with the theoretical approach of section 1.4.3.. One should also notice the non-linear shape of the velocity.

In this example, it appears that the PTO is switched on each time the sign of the velocity changes. This is a very simple criterion which could be used practically. Unfortunately, regarding the times of declutching (related to the sign of the h function), this figure does not give any useful information about what makes the controller decide to switch off the PTO and it seems difficult to find a heuristic criterion for declutching as simple as for clutching.

Let C_w be the capture width ratio of the SEAREV. It is defined as the ratio of the mean power extracted over a 600 second simulation ($\bar{P}_{PTO}$) to the wave power available in a wave front the width of the device (P_w), with:

$$P_w = 30\frac{1}{8\pi}\rho_w g^2 a^2 T_w$$

where ρ_w is the density of water, g is the gravity, a is the wave amplitude and T_w is the wave period. Figure (8) shows the capture width C_w in regular waves for pseudo-continuous control (with $N_q = 10$) and for declutching control. Three wave amplitudes are considered: 0.5, 1 and 2m. Since the system is non-linear, wave amplitude has an influence on the capture width.

As expected from the theory, one can observe that, for almost all the wave periods considered, declutching control yields a capture width at least as large as that of pseudo-continuous control. There are few exceptions to this for waves whose amplitude is 1 m and whose period is around 6.6 s or 7.6 s. It is not clear what happens for these configurations, but it may be explained by a convergence of the optimisation iterative process to a

local maximum instead of the global one. However, from an overall point of view, the theoretical result stating that declutching control can be at least equivalent to pseudo-continuous control is verified.

In this figure, one can also see the influence of the wave amplitude on the capture width. It appears that, whatever the control, the capture width decreases with the wave amplitude for short periods, but it increases for longer wave periods around 8 s. This is an interesting result as long wave periods and large amplitudes are usually correlated. It appears also that declutching control improves the capture width in small waves in comparison with pseudo-continuous control. However, it seems that the capture width with declutching control converges asymptotically to the capture width with pseudo-continuous control when the wave amplitude increases.

Figure 8. Capture width ratio of the SEAREV WEC with pseudo-continous and declutching control in regular waves The capture width is plotted against wave period. From top to bottom, the amplitude of the wave is respectively 0.5 m, 1 m and 2 m. For almost all the wave periods considered, declutching control yields an equivalent or better efficiency than pseudo-continuous control.

To assess the influence of the number N_q of levels of discretisation for the pseudo-continuous control, figure (9) shows the capture width ratio of the SEAREV WEC controlled with pseudo-control with $N_q = 1$,$N_q = 5$, $N_q = 10$ and with declutching control.

One can see that this influence is very small. For $N_q = 5$ and $N_q = 10$,

differences between the results are undistinguishable. For $N_q = 1$, which means only one level of discretisation of the PTO force, one can observe that, if the capture width is slightly reduced for periods between 6 and 8 seconds, it is surprisingly increased for periods below 6 s and between 8 s and 8.5 s. In figure (10), one can see that the amplitude of the motion with $N_q = 1$ is larger than with $N_q = 10$ for a regular wave whose period is 5.5 s and amplitude is 1 m. This leads to this increase in the capture width of the system.

From an overall point of view, it appears that declutching control leads to a higher capture width in comparison with pseudo-continuous control. However, one should notice that for pseudo-continuous control, numerous levels of discretisation N_q do not seem to have a strong influence on the capture width ratio in case of the SEAREV WEC. Practically, it is an interesting result as it shows that even the simple pseudo-continuous control calculated according to equation (12) does not need numerous of level of discretisation.

Figure 9. Capture width ratio of the SEAREV WEC with pseudo-continous control with 1, 5 and 10 levels of discretisation of the PTO force and with declutching control. Capture width values are plotted against wave period for 1 m wave amplitude. In this example, the number of discretisation levels N_q has only a small influence on the capture width ratio.

Figure 10. Time-domain simulation of the relative motion between the hull and the pendular wheel in a regular wave of 5.5 s period and 1m amplitude . Three control approaches are considered: pseudo-continuous control

with 1 and 10 levels of discretisation of the PTO force and declutching control.

2.2. Irregular waves

Figure (11) shows a 600 s time- domain simulation of the SEAREV WEC with pseudo-continuous control ($N_q = 10$) and with declutching control, in irregular waves. A Pierson Moskowitz spectrum was used for the generation of the random incident wave field with a peak period $T_p = 10$ s and a significant height $H_s = 2$ m. With these parameters, the power in the incoming wave is about 16 kW/m.

Figure 11. Time-domain simulation of the relative motion between the hull and the pendular wheel in irregular waves. Two control approaches are considered: pseudo-continuous control (solid line) and declutching control (dashed line). The peak period of the spectrum is 10 s and the significant wave height is 2 m.

In this example, the mean power production with pseudo-continuous control is 67 kW, whereas we achieved 90 kW with declutching control, i.e. an increase of more than 34%. With a pseudo-continous control with $N_q = 1$ and the same irregular wave field, the mean power production achieved is 61 kW. Declutching control therefore leads to a power production increase of more than 47% compared with pseudo-continuous control with N_q=1. Hence, one can see that declutching control seems to be a more efficient way of controlling the system in irregular waves in comparison with pseudo-continuous

control. In the plot showing the time series of the relative motion, one can see the amplification of motion achieved by declutching control compared to that associated with pseudo-continuous control.

Figure 12. Time-domain simulation of the hdyraulic PTO SEAREV WEC with declutching control in an irregular wave. The peak period of the wave is $T_p = 10$ s and the significant height $H_s = 2m$.

Figure (12) shows the behaviour of the hydraulic PTO during the first 300 seconds of simulation of the system controlled with declutching control. One can see that, after the transient associated with the starting of the system, the pressure in the HP accumulator oscillates between 220 bars and 250 bars. This leads to a useful gas volume of about 400 liters. With a PTO defined that way and a hydraulic motor displacement u_m controlled according to equation (10), one can see on the bottom figure that we achieved a satisfactory smoothing of the power delivered to the grid.

Figure 13. Ratios charts of the mean absorbed power by the SEAREV WEC with a hydraulic PTO controlled by declutching and the mean absorbed power with a pseudo-continuous control. In the top figure, the pseudo-continous control was computed with the discretisation parameter $N_q = 10$ and in bottom figure, N_q was set to one.

Figure (13) shows the ratio of the mean absorbed power by the SEAREV controlled by declutching to the mean absorbed power with a pseudo-continuous

control. Two values for the discretisation parameter N_q of the pseudo-continuous control were considered, 1 and 10. Mean power values for each sea state defined by T_z and H_s have been derived from a 600 s time-domain simulation of the motion.

Again, as expected from the theory, one can see that whatever the sea state is, the absorbed power with declutching control is always at least as high as the absorbed power with pseudo-continuous control. Like in regular waves, it appears that the ratio is close to 1 (although higher than 1) for moderate to highly energetic sea states when the wave period is within the bandwith of the system. When the wave period is far from the bandwidth of the system or in small waves, one can see that the ratio increases significantly to reach in some cases values above 2. This shows that declutching control could possibly be an alternative way for controlling the motion of wave energy converters (at least the SEAREV) in order to improve the overall energy absorption.

By comparing the top and bottom figures, one can see that, in contrast with the case of regular waves, the number of level of discretisation N_q has now a more significant influence on the capture width of the system, especially in low-energy sea states.

Conclusion

In this paper, two strategies for controlling the force applied by a hydraulic PTO were considered. The first one is a pseudo-continuous control, which consists in mimicking a continuous behaviour. The second one is a declutching control, which consists in isolating the cylinder from the high pressure side of the hydraulic circuit at precise times that are determined

using the optimal command method. The main advantage of this second control strategy is that it requires only one by-pass valve whereas the other one needs several hydraulic components, leading to a more complex system and a higher risk of failure.

By means of the optimal command method, it is shown theoretically that this declutching control is able to lead to energy absorption levels at least as high as that of pseudo-continuous control. The methodology is then applied to the practical case of the SEAREV wave energy converter, and it is shown than declutching control can even lead to a higher energy absorption both in regular and irregular waves.

However, it exists also other control strategies for hydraulic PTO, such as the latching control proposed by [Falcao 2008]. Future work will be done in order to determine which one of these strategies brings the higher capture width. One should also notice that the method used here cannot be implemented as such in the real world, as it requires the future knowledge of the excitation force. Hence, future work will be required in order to find a causal strategy to implement this control method in practical applications.

Appendix

Using equations (1), (2), (4) and (5), one can show that function $\mathbf{f}$ of equation (9) is

$$\mathbf{f}(\mathbf{X}, u_c, u_m) = \begin{pmatrix} \dot{\mathbf{Y}} \\ (\mathbf{M} + [\mu_\infty])^{-1} \left(\mathbf{F}_{ex} - [\delta]\mathbf{I} - (\mathbf{K}_H + \mathbf{K}_A)\mathbf{Y} + \mathbf{F}_{PTO}\right) \\ -u_c S_c |\dot{Y}_J| + u_m v_m \Omega \\ \gamma \dfrac{p}{V}(u_c S_c |\dot{Y}_J| - u_m v_m \Omega) \\ [\beta]\,\mathbf{I} + [\sigma]\,\dot{\mathbf{Y}} \end{pmatrix} \tag{21}$$

In the hamiltonian, equation (19), the g and h functions are given by :

$$g(\mathbf{X}, \mathbf{\Lambda}) = \mathbf{\Lambda}^t \begin{pmatrix} \dot{\mathbf{Y}} \\ (\mathbf{M} + [\mu_\infty])^{-1} \left(\mathbf{F}_{ex} - [\delta]\mathbf{I} - (\mathbf{K}_H + \mathbf{K}_A)\mathbf{Y}\right) \\ u_m v_m \Omega \\ -\gamma \dfrac{p}{V} u_m v_m \Omega \\ [\beta]\,\mathbf{I} + [\sigma]\,\dot{\mathbf{Y}} \end{pmatrix} \tag{22}$$

$$h(\mathbf{X}, \mathbf{\Lambda}) = \left(S_c(p - p_0)(\dot{Y}_J - \lambda) + \dot{Y}_J(\gamma \frac{p}{V} \Lambda_{2N_{dof}+2} - \Lambda_{2N_{dof}+1})\right) \tag{23}$$

with the λ scalar function given by :

$$\lambda = \begin{pmatrix} \Lambda_{N_{dof}+1} & \cdots & \Lambda_{2N_{dof}} \end{pmatrix} (\mathbf{M} + \mu_\infty)^{-1} \kappa \tag{24}$$

and κ a vector such as:

$$\kappa_i = \begin{cases} 1 & \text{if} \quad i = J \\ 0 & \text{else} \end{cases} \tag{25}$$

References

[Babarit 2005] Babarit, A., 2005. Optimisation hydrodynamique et contrôle optimal d'un récupérateur de l'énergie des vagues. PhD thesis, Ecole Centrale de Nantes et Université de Nantes, in French.

[Babarit 2006] Babarit, A., Clément, A.H., 2006. Optimal latching control of a wave energy device in regular and irregular waves. Applied Ocean Research vol. 28(2), pp. 77-91.

[Blondel 2008] Blondel, E., Ducrozet, G., Bonnefoy, F., Ferrant, P., 2008. Extreme wave characterization and prediction using an advanced Higher-Order Spectral (HOS) model. Proc. of the 27th Symposium on Naval Hydrodynamics, Seoul, Korea, 5-10 october 2008.

[Borne et al. 1990] Borne, P., Dauphin-Tanguy, G., Richard, J.P., Rotella, F., Zambettakis, I., 1990. Méthodes et techniques de l'ingénieur, Automatique : Commande et optimisation des processus. TECNIP-Paris.

[Budal and Falnes 1983] Budal, K., Falnes, J., 1983. Status of the norwegian wave-power buoy project. Technical report, Division of Experimental Physics, The Norwegian Institute of Technology, University of Trondhein.

[Chaplin 2007] Chaplin, R., Aggidis, G., 2007. WRASPA, Wave interactions and control in a new pitching-surge point-absorber wave energy converter. Proc. of the 7th European Wave and Tidal Energy Conference, Porto, Portugal.

[Clément 1997] Clément, A.H., 1997. Hydrodynamique instationnaire linéarisée : mise en oeuvre d'une méthode de singularités utilisant un modèle différentiel de la fonction de Green. Technical report LHN-9703, Laboratoire de Mécanique des Fluides de l'Ecole Centrale de Nantes.

[Cummins 1962] Cummins, W.E., 1962. The impulse response function and ship motions. Schiffstechnik, vol. 9, pp. 101-109.

[Duclos 2001] Duclos, G., Clément, A.H., Chatry, G., 2001. Absorption of outgoing wave in a numerical wave tank using a self-adaptative boundary condition. International Journal of Offshore and Polar Engineering 11(3), pp. 168-175.

[Falcao 2007] Falcao, A.F. de O., 2007. Modelling and control of oscillating-body wave energy converters with hydraulic power take-off and gas accumulator. Ocean Engineering vol. 34, pp 2021-2032.

[Falcao 2008] Falcao, A.F. de O., 2008. Phase control through load control of oscillating-body wave energy converters with hydraulic PTO system. Ocean Engineering vol. 35, pp. 358-366.

[Henderson 2006] Henderson, R., 2006. Design, simulation and testing of a novel hydraulic power take off system for the Pelamis wave energy converter. Renewable Energy vol. 31, pp. 271-283.

[Hoskin 1986] Hoskin, R.E, Nichols, N.K., 1986. Optimal strategies for phase control of wave energy devices. Utilization of Ocean Waves : Wave to Energy Conversion, Michael E. McCormick and Young C. Kim (Eds), pp. 184-199.

[Josset 2007] Josset, C., Babarit, A., Clément, A.H., 2007. A wave-to-wire model for the searev wave energy converter. Proceedings of the Institution of Mechanical Engineers Part M-Journal of Engineering for the Maritime Environment vol. 221(2), pp. 81-93.

[Justino 2000] Justino, P.A.P., Falcao, A.F. de O., 2000. Active relief-valve of an OWC wave energy device. Proc. of the 4th European Wave Energy Conference, pp. 295-300.

[King 1987] King, B., 1987. Time-domain analysis of wave exciting forces on ships and bodies. PhD thesis, the University of Michigan.

[Molin 2002] Molin, B., 2002. Hydrodynamique des structures offshore. Guides pratiques sur les ouvrages en mer. TECHNIP editor.

[Salter 2002] Salter, S.H., Taylor, J.R.M., Caldwell, N.J., 2002. Power conversion mechanisms for wave energy. Proceedings of the Institution of Mechanical Engineers, Part M-Journal of Engineering for the Maritime Environment, vol. 216, pp. 1-27.

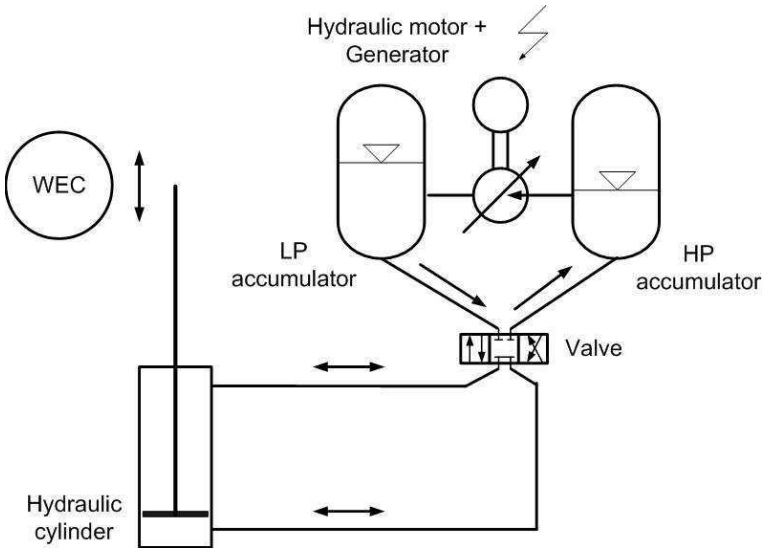

Figure 1: Schematic representation of a hydraulic PTO for wave energy conversion.

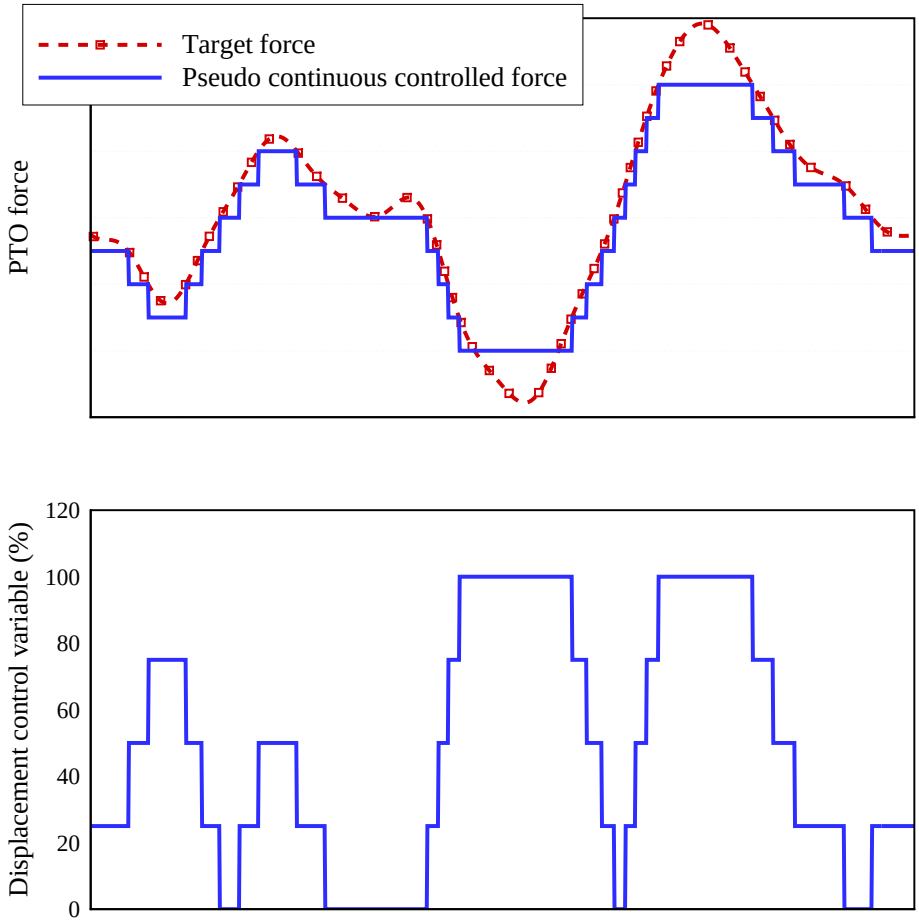

Figure 2: Principle of the pseudo-continuous control of the force of a hydraulic PTO.

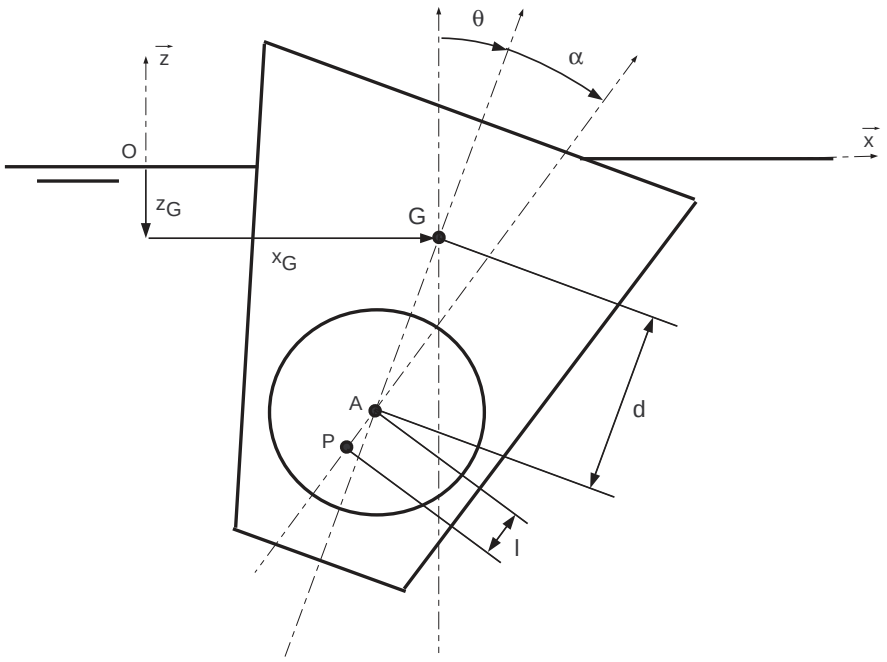

Figure 3: Schematic representation of the SEAREV wave energy converter and notations used.

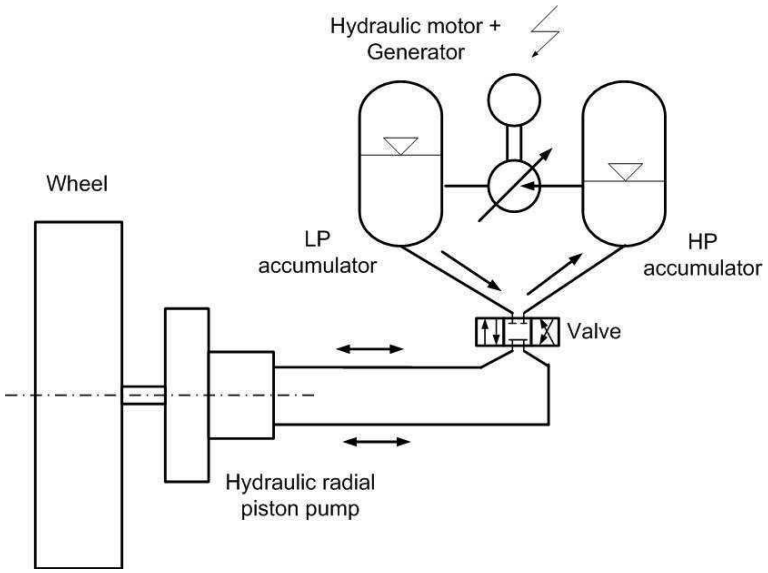

Figure 4: Schematic representation of the hydraulic PTO of the SEAREV wave energy converter. A radial piston pump is used instead of a hydraulic cylinder.

HP volume	2 m^3
Initial HP pressure	200 bars
Maximum HP pressure	350 bars
LP pressure	15 bars
S_c	402118 cm^3
v_m	701.75 cm^3
Ω	1500 rpm

Table 1: Characteristics of the SEAREV hydraulic PTO

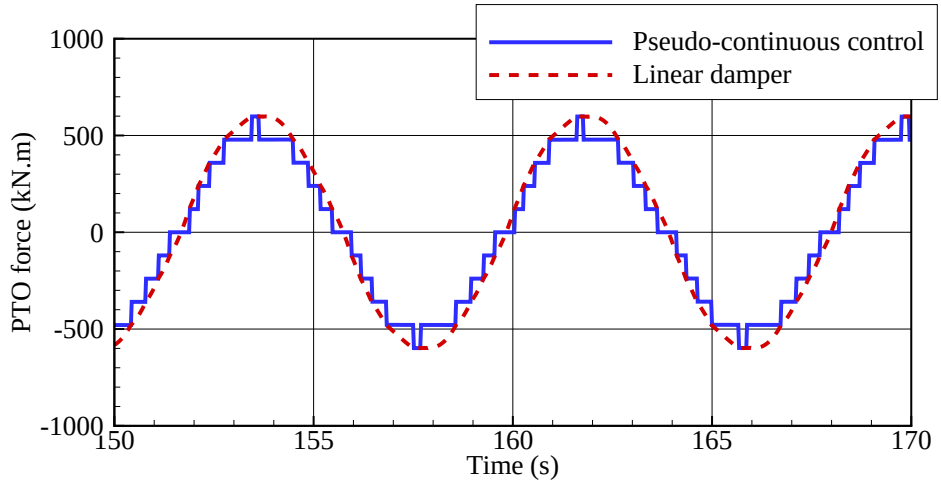

Figure 5: Comparison of the PTO force achieved with the SEAREV's hydraulic PTO controlled with the pseudo-continuous control and the PTO force achieved with a linear damper. In this example, the PTO force is discretised in 10 levels.

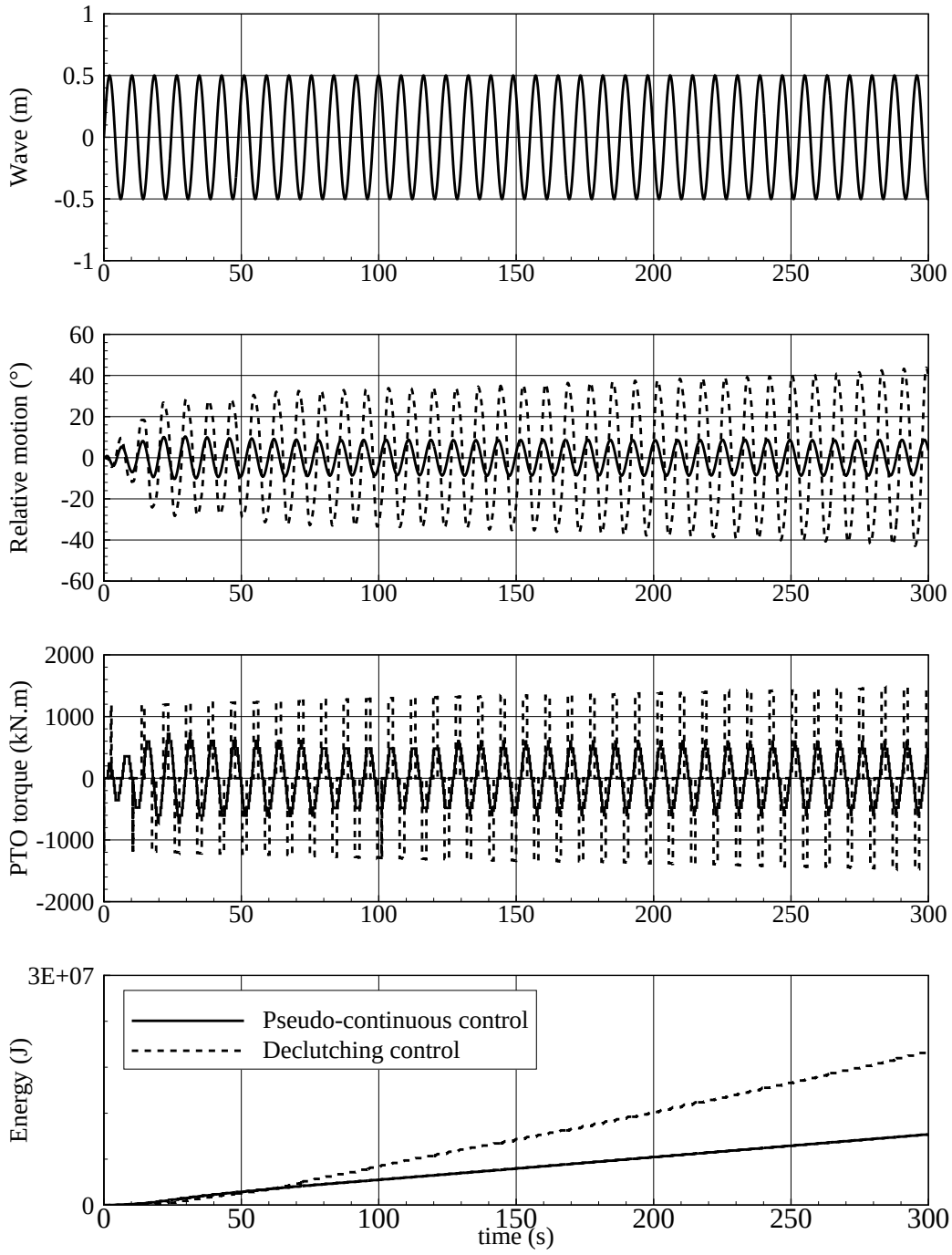

Figure 6: Time domain simulation of the motion of the SEAREV WEC with a hydraulic PTO controlled with the pseudo-continuous control (solid line) and with declutching control (dashed line). From top to the bottom, the figure shows the incoming wave, the relative motion of the wheel, the PTO force and the absorbed energy from the waves. In this example, the wave period is 8.2 seconds and the wave amplitude is 0.5 meter.

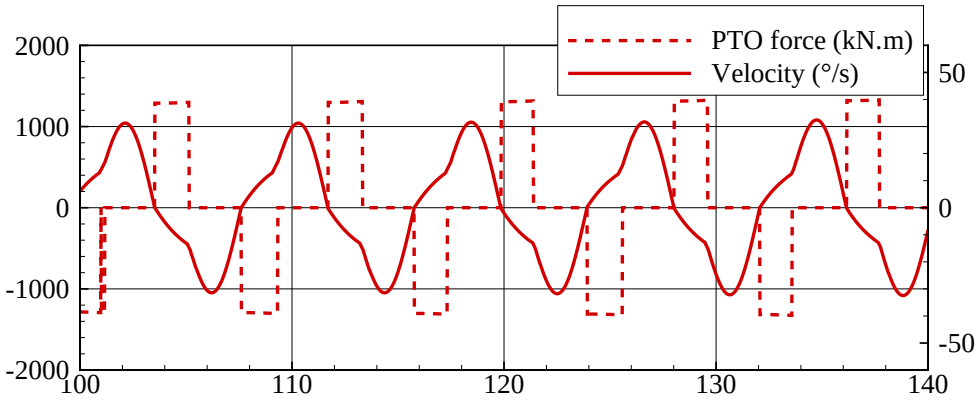

Figure 7: PTO force with declutching control and velocity of the relative motion between the hull and the pendular wheel. One can observe that each zero-crossing of the velocity leads to a change in the state of the controller from declutching to operating.

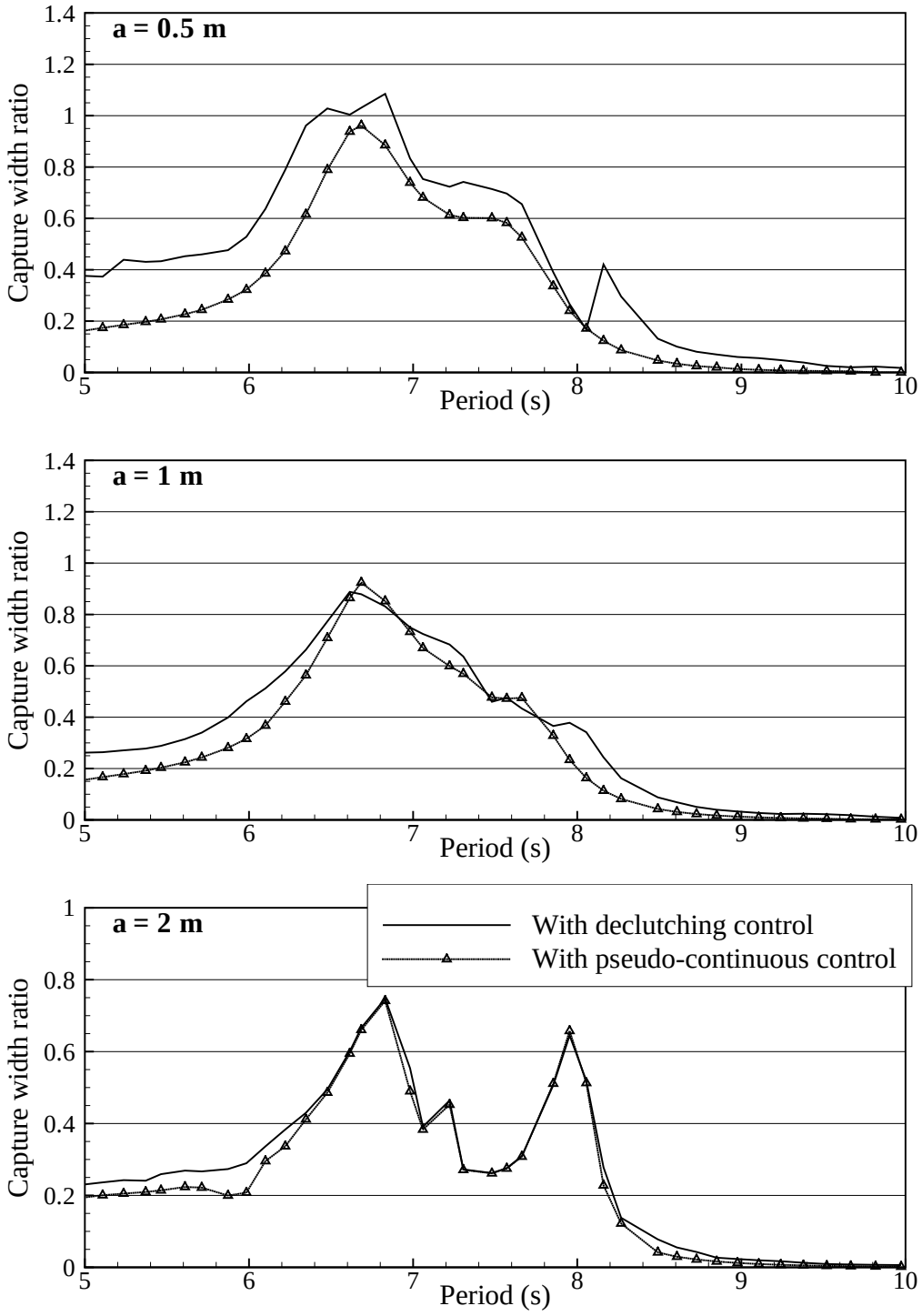

Figure 8: Capture width ratio of the SEAREV WEC with pseudo-continous and declutching control in regular waves. The capture width is plotted against wave period. From top to bottom, the amplitude of the wave is respectively 0.5 m, 1 m and 2 m. For almost all the wave periods considered, declutching control yields an equivalent or better efficiency than pseudo-continuous control.

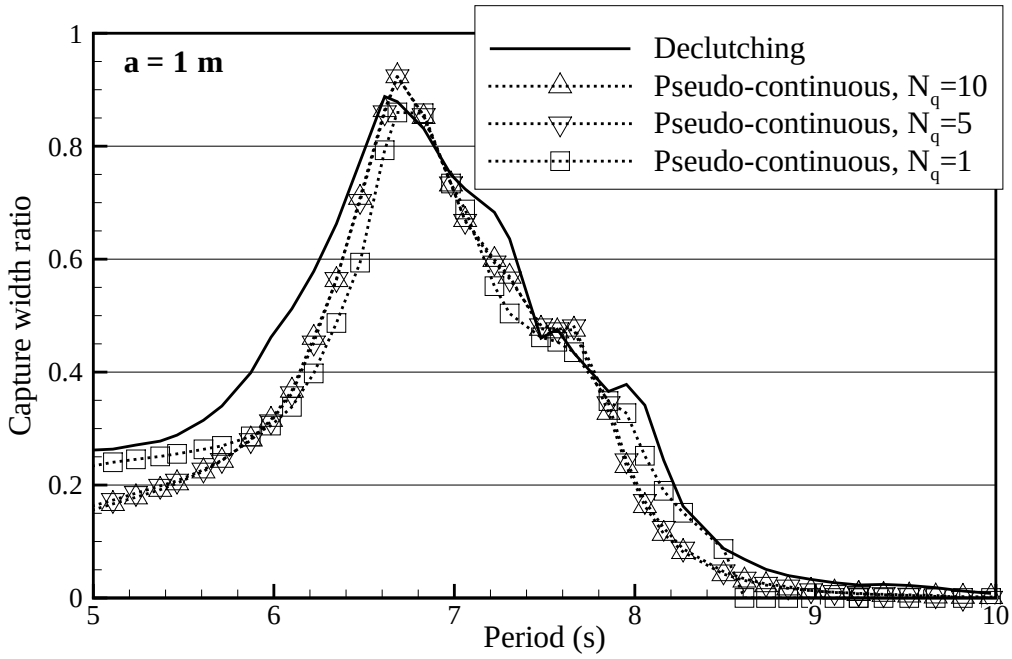

Figure 9: Capture width ratio of the SEAREV WEC with pseudo-continous control with 1, 5 and 10 levels of discretisation of the PTO force and with declutching control. Capture width values are plotted against wave period for 1 m wave amplitude. In this example, the number of discretisation levels N_q has only a small influence on the capture width ratio.

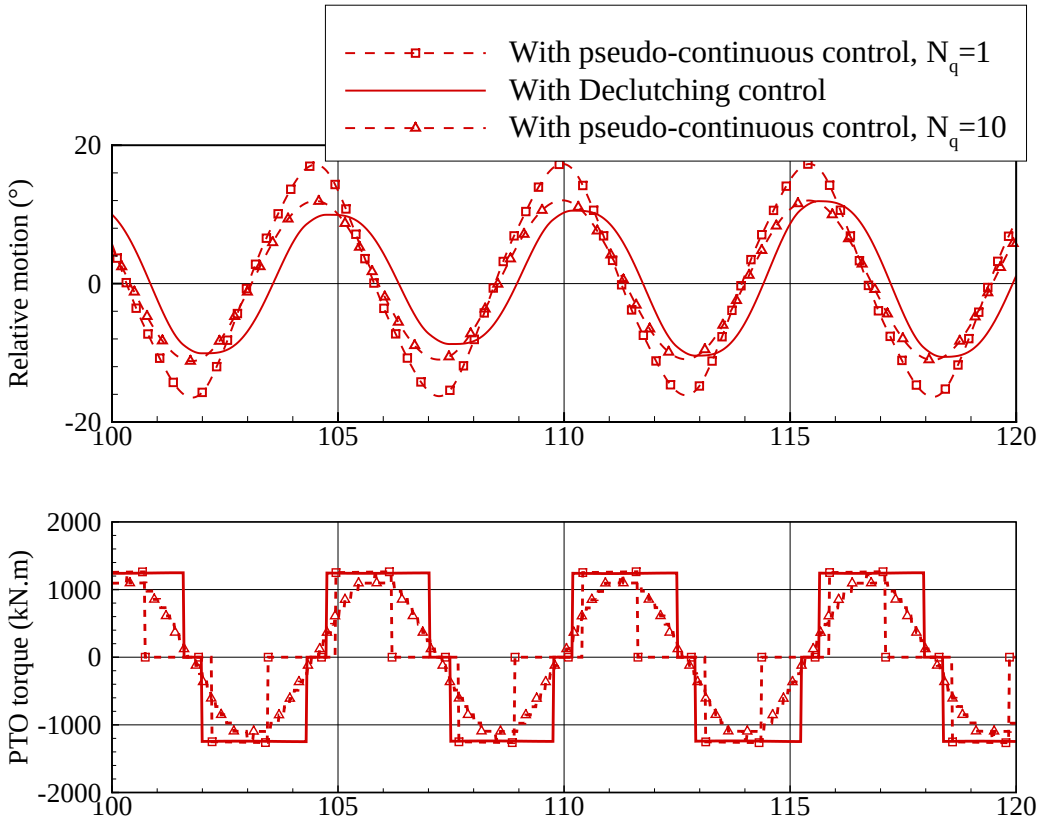

Figure 10: Time-domain simulation of the relative motion between the hull and the pendular wheel in a regular wave of 5.5 s period and 1 m amplitude . Three control approaches are considered: pseudo-continuous control with 1 and 10 levels of discretisation of the PTO force and declutching control.

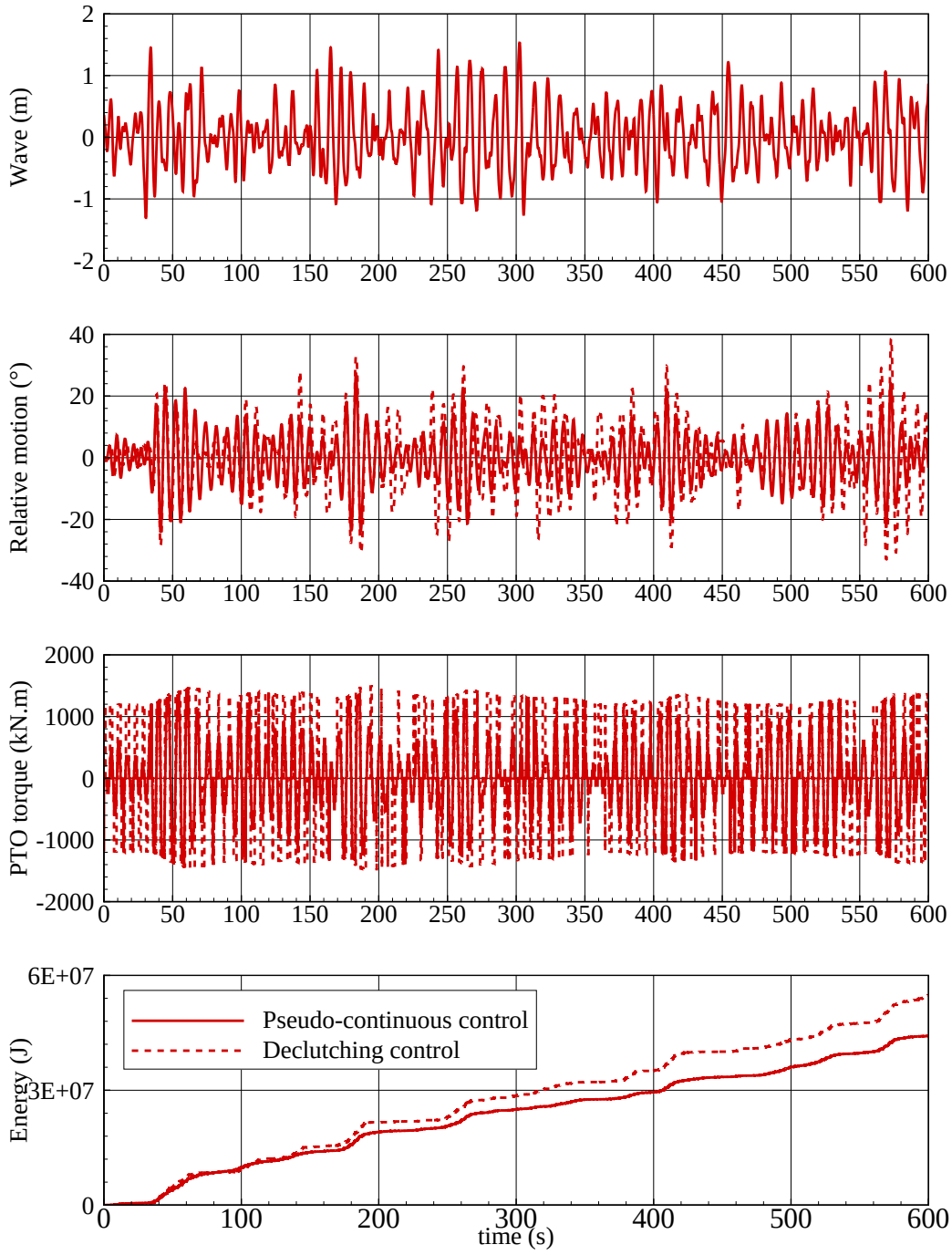

Figure 11: Time-domain simulation of the relative motion between the hull and the pendular wheel in irregular waves. Two control approaches are considered: pseudo-continuous control (solid line) and declutching control (dashed line). The peak period of the spectrum is 10 s and the significant wave height is 2 m.

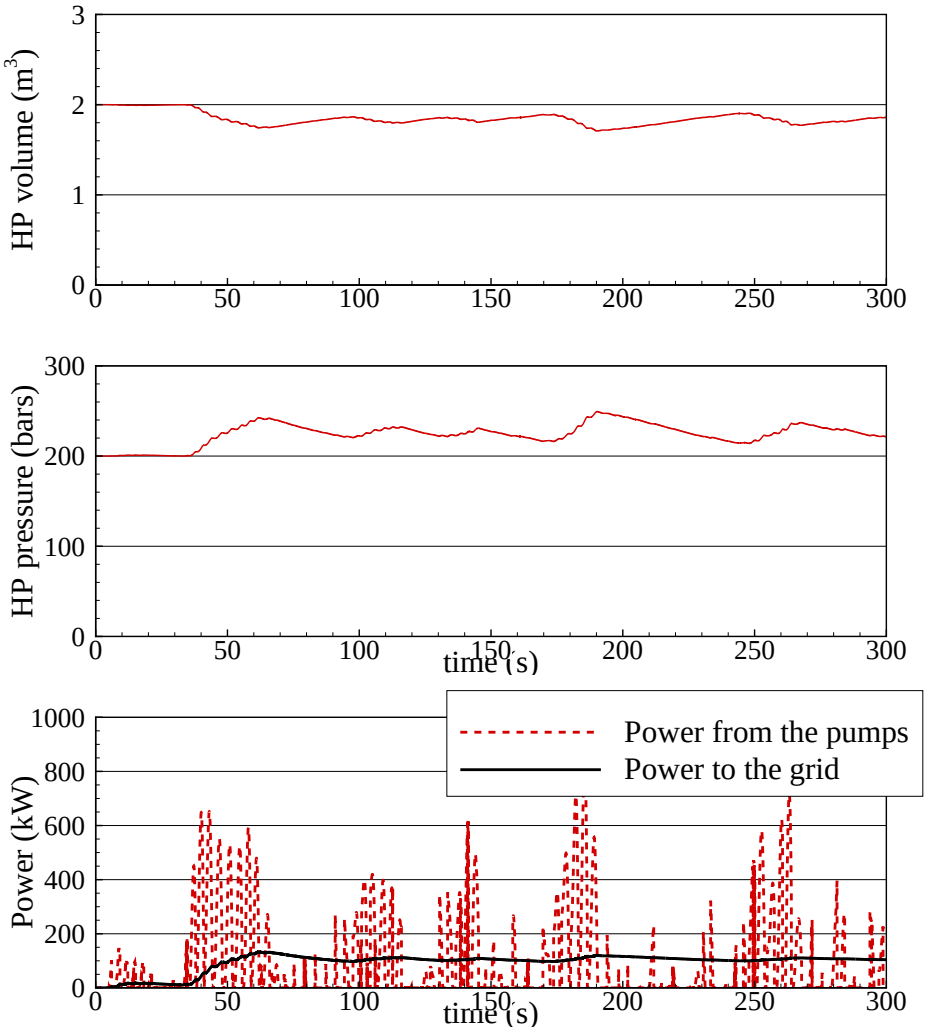

Figure 12: Time-domain simulation of the hydraulic PTO SEAREV WEC with declutching control in an irregular wave. The peak period of the wave is $T_p = 10$ s and the significant height $H_s = 2m$.

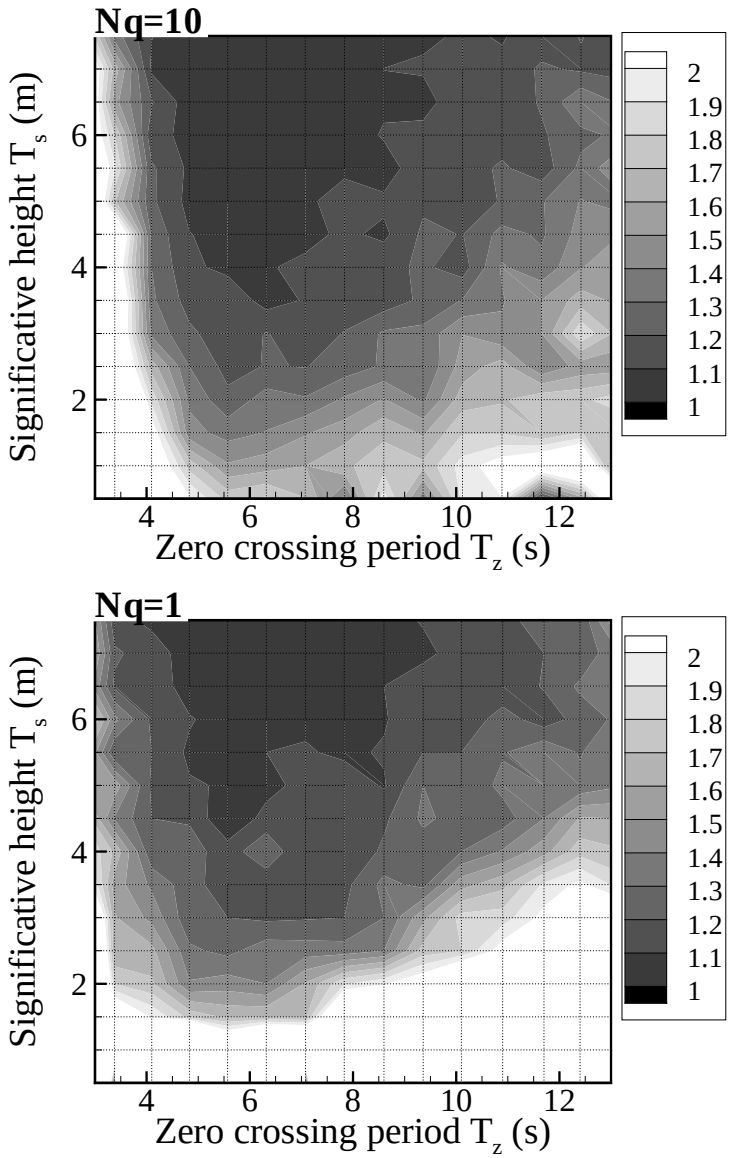

Figure 13: Ratios charts of the mean absorbed power by the SEAREV WEC with a hydraulic PTO controlled by declutching and the mean absorbed power with a pseudo-continuous control. In top figure, the pseudo-continous control was computed with the discretisation parameter $N_q = 10$ and in bottom figure, N_q was set to one.